

# Changing look quasars from tidal disruption flares

Hamsa Padmanabhan<sup>1\*</sup> and Abraham Loeb<sup>2†</sup>

<sup>1</sup> Canadian Institute for Theoretical Astrophysics, 60 St. George Street, Toronto, ON M5S 3H8, Canada

<sup>2</sup> Astronomy department, Harvard University, 60 Garden Street, Cambridge, MA 02138, USA

Accepted —. Received —; in original form —

## ABSTRACT

We explore the contributions of Tidal Disruption Events (TDEs) as potential triggers for Active Galactic Nuclei (AGN). Using the latest data available from X-ray and optical observations of high-redshift galaxies, as well as the evolution of their central supermassive black holes, we calculate the extent to which TDEs trigger AGNs as a function of their luminosities. We find that at low redshifts ( $z < 1$ ), a few percent of all AGN with bolometric luminosities  $L_{\text{Bol}} \lesssim 10^{44} \text{ erg s}^{-1}$  may be attributable to TDE triggers. However, this fraction can significantly increase at earlier cosmic times, reaching several tens of percent at  $z > 2$ , including about 20-50% of the observed population of Changing Look Quasars (CLQs). TDEs may comprise a significant fraction of the Compton-Thick (CT) AGN population at  $z > 2$ . The above findings motivate further calibration from upcoming X-ray missions and spectroscopic surveys targeting TDE-AGN.

**Key words:** galaxies: quasars: supermassive black holes - galaxies: active - galaxies: high-redshift

## 1 INTRODUCTION

Supermassive black holes (SMBHs) are known to exist at the centres of galaxies (for reviews, see, e.g., Kormendy & Ho 2013; Graham 2016). The luminosity function of Active Galactic Nuclei (AGN) constrains the growth of SMBHs that accrete at high efficiencies for extended periods of time. However, the majority of galactic nuclei are dormant, and low luminosity AGN are difficult to study due to incomplete knowledge of their accretion processes. One of the major unsolved problems in AGN research involves the fuelling of low-luminosity AGN (e.g., Martini 2004) and the growth history of SMBHs in the early universe.

A key contribution to the fuelling of AGN, especially at low luminosities, could be due to Tidal Disruption Events (TDEs). These occur when stars are deflected to a distance where they are shredded by the tidal force of the supermassive black hole when it exceeds their self-gravity (Rees 1988; Hills 1975). A significant fraction (roughly one-half) of the tidally disrupted stellar material is subsequently accreted on to the central black hole, producing a luminous flare at typically super-Eddington efficiencies (e.g., Loeb & Ulmer 1997; Kara et al. 2016). The characteristic temporal signature of a TDE is the fall-off of the initial flare with time  $t$  over a period of months to years (e.g., Strubbe & Quataert 2009) as  $t^{-5/3}$ . However, if the mass of the central black hole exceeds about  $10^8 M_{\odot}$ , a solar-type star is swallowed whole (Kesden 2012), with no radiation being produced.

So far, there have been approximately 83 observed flares that

are consistent with TDEs in AGN<sup>1</sup>, spanning the radio, optical, UV, hard X-ray and soft X-ray bands (e.g., Bloom et al. 2011; Levan et al. 2011; Cenko et al. 2012; van Velzen et al. 2011; Gezari et al. 2012). The number is expected to increase by orders of magnitude with current and upcoming surveys, e.g. the Panoramic Survey Telescope and Rapid Response System (PanSTARRS<sup>2</sup>), the Zwicky Transient Factory (ZTF<sup>3</sup>) and the Rubin Observatory Legacy Survey of Space and Time (LSST<sup>4</sup>). Detailed simulations have been used to evaluate the dominant physical processes governing TDE flares in different host galaxies (e.g., Stone & Loeb 2011, 2012; Stone & Metzger 2016; Guillochon & Ramirez-Ruiz 2015). It is believed that TDEs likely contributed to the fuelling and growth of Intermediate Mass Black Holes (IMBHs), which are considered the ‘missing link’ between stellar mass black holes and SMBHs (e.g., Sakurai et al. 2019; Fialkov & Loeb 2017). Stars swallowed whole still contributed to the growth of SMBHs above  $10^8 M_{\odot}$ . Observations of TDEs at high redshifts, therefore, provide valuable clues towards understanding the origin of the first black holes in the universe.

In this Letter, we use an empirical approach for constraining the contribution of TDEs to fuelling AGN at early times. We extend the locally inferred relations between the central black hole mass and stellar mass of the host galaxy to high redshifts (Behroozi et al. 2019; Wyithe & Loeb 2002) to study the fraction of TDEs

<sup>1</sup> A live catalog of observed TDE events is provided in <https://tde.space/statistics/host-galaxies/>

<sup>2</sup> <http://pan-starrs.ifa.hawaii.edu/public/>

<sup>3</sup> <https://www.ztf.caltech.edu/>

<sup>4</sup> <http://www.lsst.org>

\* Email: hamsa@cita.utoronto.ca

† Email: aloeb@cfa.harvard.edu

that may be expected to trigger AGN of various bolometric luminosities as a function of redshift. We explore the dependence of these results on specific AGN populations, such as Changing-Look Quasars (CLQs; e.g. [MacLeod et al. 2019](#); [Yang et al. 2018](#); [Stern et al. 2018](#); [Ross et al. 2018](#)) and Compton Thick (CT; e.g. [Malizia et al. 2009](#); [Baloković et al. 2014](#); [Marchesi et al. 2018](#)) AGN. Our results provide a useful benchmark in combining the high-redshift TDE data anticipated from upcoming time domain optical surveys (such as LSST) with those from X-ray studies of AGN populations. Further, these findings can also be used to place important constraints on the expected gravitational wave event rates associated with binary IMBH and SMBH mergers, detectable by the forthcoming *Laser Interferometer Space Antenna* (LISA<sup>5</sup>) mission.

This paper is organized as follows. In Sec. 2, we review the basic formalism connecting TDE rates to the properties of their host galaxies and central black holes. We describe the probability of TDEs arising in AGN as a function of their bolometric luminosity, accretion efficiency and host galaxy properties, and extend this framework to high redshifts. In Sec. 3, we combine the TDE probabilities with the latest compilations of absorbed and unabsorbed AGN luminosity functions ([Aird et al. 2015](#)) and the empirical evolution of the stellar masses in galaxies. We apply this to specific cases of AGN populations in Sec. 4 to estimate the contribution of TDE triggers to Changing Look Quasars (CLQs) and Compton Thick (CT) AGN. Finally, we summarize our findings and discuss future observational prospects in Sec. 5.

## 2 TDES AT HIGH REDSHIFT

The probability of TDEs arising in an AGN can be written as (e.g., [Merloni et al. 2015](#)),

$$p_{\text{TDE}}(L_{\text{bol}}) = \frac{\Gamma_{\text{TDE}} t_{\text{peak}}}{\gamma_{\text{TDE}}} \exp(-L_{\text{bol}}/L_{\text{peak}}) \left( \frac{L_{\text{bol}}}{L_{\text{peak}}} \right)^{-1/\gamma_{\text{TDE}}}, \quad (1)$$

where  $\Gamma_{\text{TDE}}$  is the rate of TDEs with peak luminosity  $L_{\text{peak}}$  occurring over a time scale  $t_{\text{peak}}$  in an AGN of bolometric luminosity  $L_{\text{bol}}$ , and  $\gamma_{\text{TDE}} = 5/3$  which is related to the decay of the flare.<sup>6</sup> The bolometric luminosity of a galaxy,  $L_{\text{bol}}$ , is related to the mass of the central supermassive black hole,  $M_{\text{BH}}$ , by the relation:

$$L_{\text{Bol}} = 1.38 \times 10^{38} \eta \left( \frac{M_{\text{BH}}}{M_{\odot}} \right) \text{erg s}^{-1} \quad (2)$$

where we have introduced the Eddington ratio  $\eta$ . We can generalize the above expression to high redshifts using the relation ([Wyithe & Loeb 2002](#), see Eq. 11 of that work) between the black hole mass and the host dark matter halo mass,  $M$  of the galaxy at redshift  $z$ :

$$M_{\text{BH}}(M, z, \mu) = A v_{c,0}(M, z)^{\mu}, \quad (3)$$

<sup>5</sup> <http://lisa.nasa.gov/>

<sup>6</sup> In place of the generic function  $f(L_{\text{bol}}/L_{\text{peak}})$  from [Merloni et al. \(2015\)](#), we have used  $f(L_{\text{bol}}/L_{\text{peak}}) = \exp(-L_{\text{bol}}/L_{\text{peak}})$  (the function  $f$  is assumed to asymptote to near-unity for  $L_{\text{bol}} \ll L_{\text{peak}}$  and drops exponentially at large  $L_{\text{bol}}$ , so this represents a natural choice.)

with  $A = 10^{-5.2}$  and  $\mu$  being a free parameter.<sup>7</sup> Thus, Eq. (2) can be rewritten as:

$$L_{\text{Bol}}(M, z, \mu, \eta) = 1.38 \times 10^{38} \eta \left( \frac{M_{\text{BH}}(M, z, \mu)}{M_{\odot}} \right) \text{erg s}^{-1} \quad (4)$$

as a function of redshift. The expression for  $L_{\text{peak}}$  is then given by (e.g., [Fialkov & Loeb 2017](#)):

$$L_{\text{peak}}(M, z, \mu, \eta) = 133 \left( \frac{M_{\text{BH}}(M, z, \mu)}{10^6 M_{\odot}} \right)^{-1.5} L_{\text{Bol}}(M, z, \mu, \eta) / \eta, \quad (5)$$

and the rate of TDEs,  $\Gamma_{\text{TDE}}$  is given by the observationally motivated fitting form (e.g., [Stone & Metzger 2016](#)):<sup>8</sup>

$$\Gamma_{\text{TDE}}(M, z, \mu) = 1.2 \times 10^{-5} \left( \frac{M_{\text{BH}}(M, z, \mu)}{10^8 M_{\odot}} \right)^{-0.247} \text{yr}^{-1}. \quad (6)$$

We also have

$$t_{\text{peak}}(M, z, \mu, \eta, \epsilon) = 0.5 \epsilon M_{\odot} c^2 / L_{\text{peak}}(M, z, \mu, \eta), \quad (7)$$

assuming a solar mass star is totally disrupted, consistently with Eq. (10) of [Fialkov & Loeb \(2017\)](#). Half the mass of the star is assumed to be accreted into the black hole which has a radiative efficiency  $\epsilon$ . Using the above ingredients, Eq. (1) can be recast as:

$$p_{\text{TDE}}(M, z; \eta, \epsilon, \mu) = \Gamma_{\text{TDE}}(M, z, \mu) t_{\text{peak}}(M, z, \eta, \mu, \eta) \times \exp(-L_{\text{bol}}(M, z, \mu, \eta) / L_{\text{peak}}(M, z, \eta, \mu)) \times \left( \frac{L_{\text{bol}}(M, z, \mu)}{L_{\text{peak}}(M, z, \eta, \mu)} \right)^{-1/\gamma_{\text{TDE}}} / \gamma_{\text{TDE}}, \quad (8)$$

with  $\eta$ ,  $\epsilon$  and  $\mu$  being adjustable parameters.<sup>9</sup> Fig. 1 plots the quantity  $p_{\text{TDE}}$  against  $L_{\text{bol}}$  for various redshifts, assuming  $\eta = 0.01$ ,  $\mu = 4$ ,  $\epsilon = 0.1$  and a host halo mass range of  $\{10^{11}, 10^{15}\} M_{\odot}$ . The figure shows that for a given  $L_{\text{bol}}$ , the  $p_{\text{TDE}}(L_{\text{bol}})$  is relatively insensitive to  $z$  (since it has very little dependence on the parameter  $\eta$  and thus on the black hole mass  $M_{\text{BH}}$ , e.g. [Merloni et al. \(2015\)](#).) We also note the characteristic drop-off of this function above bolometric luminosities  $\gtrsim 10^{45}$  erg/s, which arises due to the direct stellar capture by black holes above the corresponding masses  $M_{\text{BH}} \sim 10^8 M_{\odot}$  (e.g., [Kesden 2012](#)). The duration  $t_{\text{peak}}$  as a function of  $L_{\text{bol}}$  for these parameters and halo mass ranges from about 0.1 to a few years.

## 3 FRACTION OF TDES IN AGN

Given the rates for TDEs occurring in AGN as calculated in the previous section, we can now compute the probability of TDEs occurring in different AGN populations in a particular bolometric luminosity interval as a function of redshift. To do this, we use

<sup>7</sup> Observations suggest the value of  $\mu \sim 4 - 5$ , we illustrate results for a fiducial  $\mu = 4$  here, but the present results are only weakly affected by changes in  $\mu$ .

<sup>8</sup> We are making the implicit assumption that the TDE rate is influenced by physical processes that are not expected to change with redshift. The latest compilations connecting TDE rates to their observed host galaxy properties (e.g., [French et al. 2020](#)) find that a TDE rate of  $\sim 10^{-5}$  per year per galaxy is well borne out by recent data.

<sup>9</sup> Note that the  $p_{\text{TDE}}$  as calculated has a very weak dependence on  $\eta$  ( $\propto \eta^{-0.047}$ ).

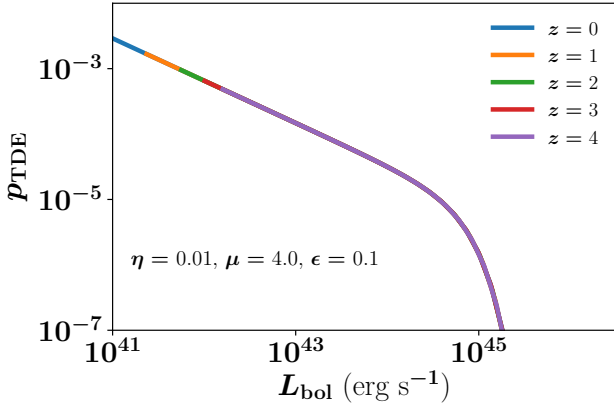


**Figure 1.** The probability of TDE,  $p_{\text{TDE}}$  arising in AGN as a function of their bolometric luminosity,  $L_{\text{bol}}$  for a population having  $\eta = 0.01$ ,  $\mu = 4$  and  $\epsilon = 0.1$  at various redshifts.

the definition of  $p_{\text{AGN}}$ , used in, e.g., Merloni et al. (2015), which measures the probability of AGN with a specified bolometric luminosity,  $L_{\text{bol}}$ , arising in host galaxies with a given total stellar mass ( $M_*$ ) at redshift  $z$ . This is given by,

$$p_{\text{AGN}} = \phi_{\text{AGN}}(L_{\text{bol}}) / \phi_{\text{SMF}}(M_* | L_{\text{bol}}), \quad (9)$$

where  $\phi_{\text{AGN}}$  is the AGN luminosity function, typically given by a Schechter or double power law form<sup>10</sup> (e.g. Aird et al. (2015)), shown in the top panel of Fig. 2) and  $\phi_{\text{SMF}}$  is the stellar mass function of the host galaxy. In order to generalize  $\phi_{\text{SMF}}$  to high redshifts, we use the average relation between the total stellar mass and host halo mass of a galaxy,  $M_*(M, z)$  (derived empirically by Behroozi et al. (2019) at various redshifts) converted into an equivalent bolometric luminosity of the central AGN by using Eq. (4), via the black hole - halo mass relation, Eq. (3). Thus, we arrive at an equivalent stellar mass function expressible in terms of the bolometric luminosity of the central AGN,  $\phi_{\text{SMF}}(L_{\text{bol}}, z)$ , for a given  $\eta$  and  $\mu$ . Using the latest results from the WINGS (at  $z \sim 0$ ; Vulcani et al. 2011) and the COSMOS (at  $z \sim 0.2-5$ ; Davidzon et al. 2017) for the stellar mass function, we obtain the curves in the lower panel of Fig. 2 for  $\phi_{\text{SMF}}(L_{\text{bol}}, z)$ , assuming  $\eta = 0.01$  and  $\mu = 4$ . These show that the ‘knee’ of the stellar mass function gradually shifts to higher bolometric luminosities at higher redshifts, since a given stellar mass  $M_*$  corresponds to a larger  $M_{\text{BH}}$  (and thus a larger  $L_{\text{bol}}$ ) as  $z$  increases.

Since  $L_{\text{bol}}$  can be expressed as a function of halo mass and redshift as in Eq. (4), we can thus equivalently rewrite Eq. (9) as:

$$p_{\text{AGN}}(M, z; \mu, \eta) = \phi_{\text{AGN}}(M, z, \mu, \eta) / \phi_{\text{SMF}}(M, z, \mu, \eta), \quad (10)$$

in a manner similar to that of  $p_{\text{TDE}}$  calculated in the previous section (Eq. (8)). Eqs. 8 and 9 can now be used to calculate the fraction of TDE-triggered AGNs as a function of their host halo and galaxy properties:

$$p(\text{TDE}|\text{AGN}) = p_{\text{TDE}}(M, z; \eta, \epsilon, \mu) / p_{\text{AGN}}(M, z; \mu, \eta), \quad (11)$$

where the numerator on the right-hand side denotes the probability of TDEs occurring in AGN as calculated in the previous section

<sup>10</sup> The X-ray luminosity for 2 - 10 keV is converted to bolometric luminosity by using the bolometric correction  $\log L_X = (\log L_{\text{bol}} - 23.04) / 0.52$  from Runnoe et al. (2012).

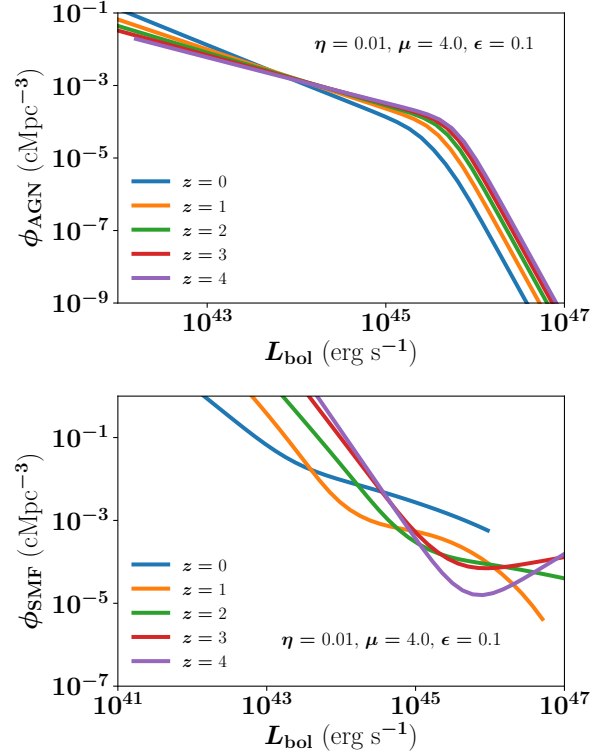


**Figure 2.** Top panel: Observed AGN luminosity function,  $\phi_{\text{AGN}}(L_{\text{bol}})$  at different redshifts from the X-ray data of Aird et al. (2015) and using the bolometric correction of Runnoe et al. (2012) to convert X-ray luminosity to bolometric luminosity. Lower panel: Stellar mass functions compiled from the latest WINGS (Vulcani et al. 2011,  $z \sim 0$ ) and COSMOS (Davidzon et al. 2017,  $z \sim 0.2-5$ ) survey data converted into the equivalent  $\phi_{\text{SMF}}(L_{\text{bol}})$  by using the relation  $M_* - M_{\text{BH}}$  (assuming  $\mu = 4$ ) and  $M_{\text{BH}} - L_{\text{bol}}$  (assuming  $\eta = 0.01$ ).

(Eq. (8)), or, equivalently, the joint probability of TDEs and AGN, and the denominator measures the probability of AGN occurring in host galaxies at different redshifts. For a fiducial AGN population having  $\eta = 0.05$  (e.g. Lusso et al. 2012),  $\mu = 4$  and  $\eta = 0.1$ , this quantity is plotted in Fig. 3.

At low luminosities ( $L_{\text{bol}} \sim 10^{43}$  erg/s), TDEs may account for a few to a few ten percent of AGN at  $z \sim 0-1$ , consistent with observational estimates. However, as Fig. 3 shows, this number could reach a significant fraction of low-luminosity AGN at higher redshifts, which can be tested by future data. In this and subsequent figures, the fractions plotted are indicative; physical processes are expected to limit the values to below unity in realistic scenarios.

#### 4 TDES IN DIFFERENT AGN POPULATIONS

Thus far, we have considered the occurrences of TDEs in fiducial AGNs with specified host galaxy properties, which are assumed to be representative of a generic AGN population at various redshifts. Next, we briefly consider the occurrence of TDEs in a couple of specific classes of AGN, namely (i) Changing-Look AGN (or Changing Look Quasars, CLQs; e.g. Yang et al. 2018; MacLeod et al. 2019; Ross et al. 2018; Stern et al. 2018) and (ii) Compton-Thick AGN or CT AGN (e.g. Baloković et al. 2014; Malizia et al. 2009; Marchesi et al. 2018).

The origin of the so-called ‘changing-look’ phenomena in

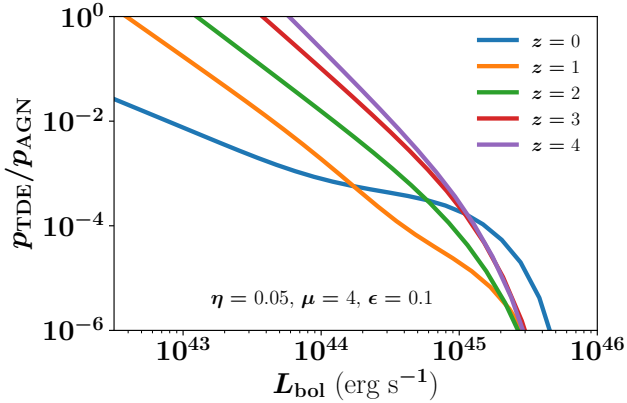


**Figure 3.** Ratio  $p_{\text{TDE}}/p_{\text{AGN}}$  for a fiducial AGN population having an Eddington ratio of 0.05, the radiative efficiency  $\epsilon = 0.1$  and the exponent of the BH mass - virial velocity relation being  $\mu = 4$ .

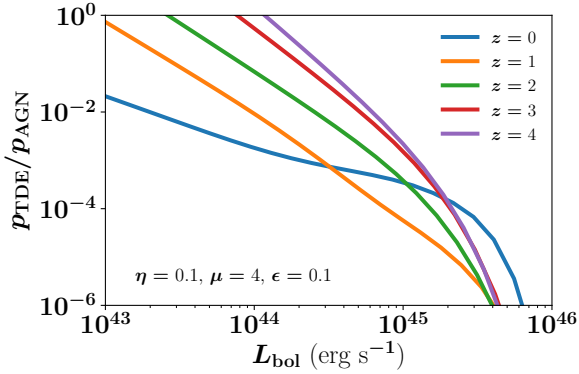


**Figure 4.** Ratio  $p_{\text{TDE}}/p_{\text{AGN}}$  for an assumed population having an Eddington ratio of 0.1 (characteristic of low- $z$  changing look quasars), the exponent of the BH mass - virial velocity relation being  $\mu = 4$  and the radiative efficiency  $\epsilon = 0.1$ .

AGN, in which a luminous quasar dims significantly over a timescale of  $< 10$  years, is currently unknown. AGN classified as changing-look (CL) have been currently discovered in the local universe up to a highest redshift of  $z \sim 2$ . More than 20% (MacLeod et al. 2019) of quasars with  $L_{\text{bol}} > 10^{44}$  erg s $^{-1}$ , and 30-50% of quasars with  $L_{\text{bol}} \sim 10^{45} - 10^{47}$  erg s $^{-1}$  (Rumbaugh et al. 2018) are found to fall into this category. CLQs typically have Eddington ratios around 0.1 (e.g., Fig. 14 of Graham et al. (2019)).

Using the machinery developed in the previous sections, we can now estimate how many of the low- $z$  CLQ discovered so far may be accounted for as TDE-triggered AGN. The  $p_{\text{TDE}}/p_{\text{AGN}}$  curve for an Eddington ratio  $\eta \sim 0.1$  corresponding to the CL observations is plotted in Fig. 4. We find that at  $z \sim 1$ , a maximum of  $\sim 10\%$  of the AGN with  $L_{\text{bol}} > 10^{44}$  erg s $^{-1}$  may originate from TDE-triggerers, which thus represents about 20 – 50% of the observed CLQ abundance.<sup>11</sup>

On the other hand, at higher redshifts, there is evidence to indicate a much larger fraction of TDE-triggered AGN in the CLQ

<sup>11</sup> The  $t_{\text{peak}}$  timescales for the  $L_{\text{bol}}$  values for  $\eta \sim 0.01 - 0.1$  range from about 0.03 to a few ten years over  $z \sim 0 - 4$ , which are broadly consistent with the changing-look timescales expected from the literature.

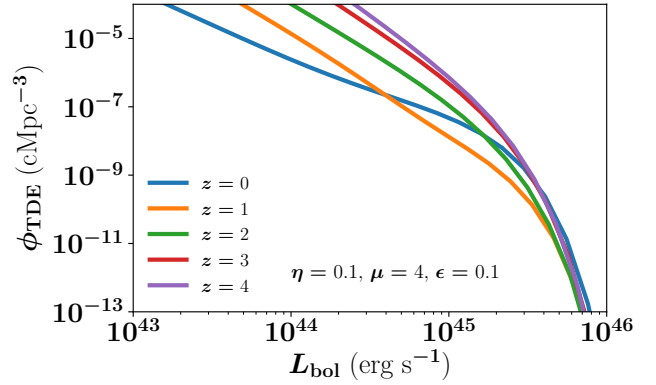


**Figure 5.** Predicted luminosity function of TDE-triggered AGN,  $\phi_{\text{TDE}} \equiv p_{\text{TDE}} \times \phi_{\text{SMF}}$  for an assumed population having an Eddington ratio of 0.1 (characteristic of low- $z$  changing look quasars), the exponent of the BH mass - virial velocity relation being  $\mu = 4$  and the radiative efficiency  $\epsilon = 0.1$ . The predicted  $\phi_{\text{TDE}}$  serves as a lower limit on the luminosity function of changing look quasars, assuming their intrinsic parameters remain redshift independent.

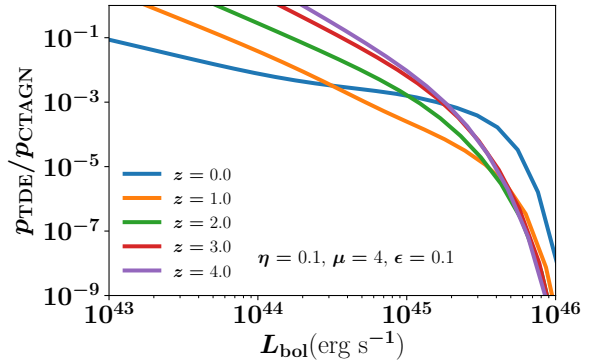


**Figure 6.** The probability of CT AGN hosting a TDE at various redshifts. The Eddington ratio is assumed to be 0.1, the exponent of the BH mass - virial velocity relation is  $\mu = 4$  and the radiative efficiency  $\epsilon = 0.1$ .

population. The first CLQs at  $z > 2$  which have recently been discovered (Ross et al. 2019) have Eddington ratios of  $\eta > 0.05$ . Upcoming experiments such as the Dark Energy Spectroscopic Instrument (DESI; DESI Collaboration et al. 2016) and LSST will enable stringent constraints on this population at higher redshifts. Assuming the intrinsic parameters of the population do not change significantly with redshift, we predict a ‘TDE luminosity function’,  $\phi_{\text{TDE}} \equiv p_{\text{TDE}} \times \phi_{\text{SMF}}$  as shown in Fig. 5. This function provides a lower limit on the abundance of CLQs at high- $z$  which may be exclusively triggered by TDEs.

It is possible that most TDE AGN have a thick envelope of gas around them, making them detectable in X-rays but not in optical-UV. This population may thus appear as CT AGN. Adopting the luminosity function of CT AGN (as a function of the absorbed AGN fraction) from Aird et al. (2015), we calculate the ratio  $p_{\text{TDE}}/p_{\text{CTAGN}}$  which is plotted in Fig. 6. We find that the TDE fraction in CT AGN can be a few ten percent around  $L_{\text{bol}} \sim 10^{43}$  erg s $^{-1}$  at redshifts  $z \sim 1$ . At higher redshifts, it may reach a significant fraction of the CT AGN population. In all cases, it drops sharply as expected after  $L_{\text{bol}} \sim 10^{46}$  erg s $^{-1}$ .

## 5 DISCUSSION

We have considered the fraction of AGN which may arise from tidal disrupted events (TDEs) at low and high redshifts. In so doing, we have extended the locally observed relations connecting the rates of TDEs to the masses of the central supermassive BH hosts of the AGN, to high redshifts using the inferred evolution of the black - hole mass - bulge mass relation from Wyithe & Loeb (2002). We have estimated the fraction of TDEs occurring in different AGN populations by relating the masses of the central black holes fuelling the AGN to the stellar masses of their host galaxies, and extending this connection to higher redshifts using the empirically derived stellar mass evolution from Behroozi et al. (2019). For a fiducial AGN population having an average Eddington ratio of  $\eta = 0.05$ , a radiative efficiency of  $\epsilon = 0.1$  and an assumed black hole - velocity dispersion exponent of 4, we find that TDEs are able to account for a few percent of all AGN with bolometric luminosities  $L_{\text{Bol}} \gtrsim 10^{43} \text{ erg s}^{-1}$  at  $z \sim 0 - 1$ , but may reach greater than a few tens of percent at  $z > 2$ .

It is also of interest to explore to what extent specific AGN populations are likely to be the result of TDE triggers at low and high redshifts. Two examples of such populations are the so-called Changing-Look AGN (or Changing Look Quasars, CLQs) and Compton-Thick AGN (or CT AGN). On applying the above formalism to these populations, we found that a maximum of about ten percent of the observed CLQ AGN (having  $L_{\text{Bol}} > 10^{44} \text{ erg s}^{-1}$ ) may be consistent with a TDE-triggered origin at  $z \sim 1$ , though this fraction may increase rapidly at higher redshifts, to  $\gtrsim 50\%$  at  $z \gtrsim 2$ . We also find that in the TDE fraction may be about a few percent to a few tens of percent of CT AGN with  $L_{\text{Bol}} \gtrsim 10^{43} \text{ erg s}^{-1}$  at redshifts  $z < 1$ , but may again account for more than 50% of this population at  $z \gtrsim 2$ .

In Fig. 10 of Lanzuisi et al. (2018), an analysis of CT AGN carried out from the *Chandra*-COSMOS legacy survey finds that the fraction of CT AGN increases with increasing redshifts, and the merger fraction in CT AGN increases with increasing luminosities and redshifts. Interestingly, a sharp rise in the “fraction of merged/disturbed morphology” in different AGN (CT/non-CT) occurs above  $L_{\text{Bol}} > 10^{46} \text{ erg s}^{-1}$ . This may be attributable to the non-TDE triggered AGN being triggered primarily by mergers, with the merger fraction increasing sharply once the maximum black hole mass of  $10^8 M_{\odot}$  is reached, consistently with our results in Fig. 6.

The present results serve as a useful benchmark for calibrating future simulations of the physical processes giving rise to TDEs in AGN at high redshifts, and their inferred contributions in various AGN populations. Current and future surveys, e.g. the *Athena*<sup>12</sup> and *Lynx*<sup>13</sup> missions that target different AGN populations will be able to place stringent constraints on the CT AGN fractions at high redshifts, and combining this data with the findings of spectroscopic surveys such as the LSST and DESI will allow us to better quantify the contributions of TDEs as AGN triggers at these epochs. The above formalism will in turn enable the most precise constraints thus far on the evolution of the central black hole - halo mass relation of the host galaxies at high redshifts. Further, the forthcoming detections of TDEs will unveil the as-yet poorly understood processes governing the growth of IMBHs and SMBHs, whose mergers are expected to constitute the primary gravitational

wave event triggers detectable by the forthcoming LISA observatory.

## 6 ACKNOWLEDGEMENTS

The work of AL was supported in part by the Black Hole Initiative at Harvard University, which is funded by grants from the JTF and GBMF.

## REFERENCES

- Aird J., Coil A. L., Georgakakis A., Nandra K., Barro G., Pérez-González P. G., 2015, *MNRAS*, **451**, 1892
- Baloković M., et al., 2014, *The Astrophysical Journal*, **794**, 111
- Behroozi P., Wechsler R. H., Hearin A. P., Conroy C., 2019, *MNRAS*, **488**, 3143
- Bloom J. S., et al., 2011, *Science*, **333**, 203
- Cenko S. B., et al., 2012, *ApJ*, **753**, 77
- DESI Collaboration et al., 2016, arXiv e-prints, p. arXiv:1611.00036
- Davidzon I., et al., 2017, *A&A*, **605**, A70
- Fialkov A., Loeb A., 2017, *MNRAS*, **471**, 4286
- French K. D., Wevers T., Law-Smith J., Graur O., Zabludoff A. I., 2020, The Host Galaxies of Tidal Disruption Events (arXiv:2003.02863)
- Gezari S., et al., 2012, *Nature*, **485**, 217
- Graham A. W., 2016, Galaxy Bulges and Their Massive Black Holes: A Review. p. 263, doi:10.1007/978-3-319-19378-6\_11
- Graham M. J., et al., 2019, *Monthly Notices of the Royal Astronomical Society*
- Guillochon J., Ramirez-Ruiz E., 2015, *The Astrophysical Journal*, **809**, 166
- Hills J. G., 1975, *Nature*, **254**, 295
- Kara E., Miller J. M., Reynolds C., Dai L., 2016, *Nature*, **535**, 388
- Kesden M., 2012, *Phys. Rev. D*, **85**, 024037
- Kormendy J., Ho L. C., 2013, *ARA&A*, **51**, 511
- Lanzuisi G., et al., 2018, *MNRAS*, **480**, 2578
- Levan A. J., et al., 2011, *Science*, **333**, 199
- Loeb A., Ulmer A., 1997, *ApJ*, **489**, 573
- Lusso E., et al., 2012, *Monthly Notices of the Royal Astronomical Society*, **425**, 623
- MacLeod C. L., et al., 2019, *ApJ*, **874**, 8
- Malizia A., Stephen J. B., Bassani L., Bird A. J., Panessa F., Ubertini P., 2009, *MNRAS*, **399**, 944
- Marchesi S., Ajello M., Marcotulli L., Comastri A., Lanzuisi G., Vignali C., 2018, *ApJ*, **854**, 49
- Martini P., 2004, in Storchi-Bergmann T., Ho L. C., Schmitt H. R., eds, IAU Symposium Vol. 222, The Interplay Among Black Holes, Stars and ISM in Galactic Nuclei. pp 235–241 (arXiv:astro-ph/0404426), doi:10.1017/S1743921304002170
- Merloni A., et al., 2015, *MNRAS*, **452**, 69
- Rees M. J., 1988, *Nature*, **333**, 523
- Ross N. P., et al., 2018, *MNRAS*, **480**, 4468
- Ross N. P., Graham M. J., Calderone G., Ford K. E. S., McKernan B., Stern D., 2019, arXiv e-prints, p. arXiv:1912.05310
- Rumbaugh N., et al., 2018, *ApJ*, **854**, 160
- Runnoe J. C., Brotherton M. S., Shang Z., 2012, *MNRAS*, **422**, 478
- Sakurai Y., Yoshida N., Fujii M. S., 2019, *Monthly Notices of the Royal Astronomical Society*, **484**, 4665–4677
- Stern D., et al., 2018, *ApJ*, **864**, 27
- Stone N., Loeb A., 2011, *MNRAS*, **412**, 75
- Stone N., Loeb A., 2012, *MNRAS*, **422**, 1933
- Stone N. C., Metzger B. D., 2016, *MNRAS*, **455**, 859
- Strubbe L. E., Quataert E., 2009, *MNRAS*, **400**, 2070
- Vulcani B., et al., 2011, *MNRAS*, **412**, 246
- Wyithe J. S. B., Loeb A., 2002, *ApJ*, **581**, 886
- Yang Q., et al., 2018, *ApJ*, **862**, 109
- van Velzen S., K rding E., Falcke H., 2011, *MNRAS*, **417**, L51

<sup>12</sup> <https://www.the-athena-x-ray-observatory.eu/>

<sup>13</sup> <https://www.lynxobservatory.com/>